Electrochemical and Solid-State Letters, **8** (2) G57-G59 (2005)
1099-0062/2004/8(2)/G57/3/$7.00 © The Electrochemical Society, Inc.

Room-Temperature Preperation of InGaAsN Quantum Dot Lasers Grown by MOCVD

Q. Gao,[z] M. Buda, H. H. Tan, and C. Jagadish*

Department of Electronic Materials Engineering, Research School of Physical Sciences and Engineering, The Australian National University, Canberra, ACT 0200, Australia

An InGaAsN single-layer quantum dot (QD) laser structure was grown on GaAs substrates by metalorganic chemical vapor deposition (MOCVD). The ridge-waveguide edge emitting laser diodes (LD) were fabricated and characterized. We demonstrate room-temperature operation of InGaAsN QD lasers with an emission wavelength of 1078 nm. Electroluminescence spectra as a function of injection current showed that InGaAsN QD LDs lased from an excited QD state at room temperature. The evidence for QD-related absorption was obtained from the comparison of photocurrent spectra between a reference InGaAs QW and the InGaAsN QD structures.
 [DOI: 10.1149/1.1848293]

Manuscript submitted July 29, 2004; revised manuscript received September 23, 2004. Available electronically December 23, 2004.

Long-wavelength (1.3 or 1.55 μm) semiconductor laser diodes are key devices for long-haul optical fiber communications and have attracted much attention in recent years due to their zero dispersion and minimal absorption in currently installed silica fibers. In particular, InGaAsN/GaAs QW lasers have been intensively studied due to their higher characteristic temperature, easier fabrication, and lower cost compared with InGaAsP/InP based long-wavelength lasers.[1-5] To date, a number of InGaAsN QW lasers have been demonstrated which showed characteristic temperatures up to 215 K[2] and threshold current densities as low as 200 A/cm^2.[5]

However, the lasing wavelength of most of these QW based lasers has been limited to around 1.3 μm, due to the difficulty of growing high-quality InGaAsN/GaAs QW structures with high composition of In or N. It is well known that quantum-dot (QD) lasers were anticipated to have many advantages over their QW counterparts, such as largely extended emission wavelength, decreased transparency current density, increased material and differential gain, and a large characteristic temperature.[6,7] Some of these predictions have been verified today on In(Ga)As QD devices, such as long-wavelength (~1.3 μm) emission,[8,9] low threshold current density,[10] high differential gain,[11] and high characteristic temperature.[12] Therefore, an alternate approach to extend the wavelength and improve the performance of laser devices based on the InGaAsN active region is to use the self-assembled InGaAsN-QD structure. Compared with a large amount of research on InGaAsN/GaAs QW lasers, very few studies on InGaAsN quantum dot (QD) lasers have been published.[13] Recent reports have shown the operational InGaAsN QD laser devices at liquid nitrogen temperature[13] and the photoluminescence (PL) emission in the 1.5 μm range from the InGaAsN QDs[14,15] indicating that the InGaAsN QDs are very promising for long-wavelength laser devices. In this paper, we demonstrate a room-temperature (RT) operating InGaAsN QD laser grown by metalorganic chemical vapor deposition (MOCVD). The lasing emission is attributed to the excited-state transition in QDs.

Experimental

To minimize the threshold current for the InGaAsN QD laser, a small spot size laser structure was designed with $d/\Gamma = 0.3$ μm (where d is the thickness of the active layer and Γ is the confinement factor). In addition, to reduce the blueshift of the emission wavelength due to the intermixing in the QDs[16] during growth of the top AlGaAs cladding layer, a thin p-cladding layer consisting of a 0.45 μm thick $Al_{0.40}Ga_{0.60}As$ layer was adopted. Details of the structure design were described in Ref. 17. The whole laser structure was grown in two separate MOCVD reactors at 76 Torr to avoid the possible reaction between Al and N. Arsine and dimethylhydrazine were used as the group V sources, while trimethylgallium, trimethyl aluminum and trimethylindium were used as the group III sources. The whole growth can be divided into three steps. The first and the third steps were carried out in an AIXTRON 200 reactor, while the second step was carried out in a modified Thomson-Swan reactor. In the first growth step (Part I), the growth temperature was maintained at 750°C. In the second growth step (Part II), GaAs was grown firstly at 600°C. The wafer was then cooled down to 550°C to commence the growth of 12 monolayers of InGaAsN QDs, in which the nominal In content and N content were 40 and 3%, respectively. The N content is estimated from a reference GaAsN epilayer grown in the same condition. However, due to the incorporation of In, the N content in InGaAsN could be reduced.[18,19] The growth temperature was then ramped back to 600°C during growth of the capping GaAs layer to finish the second growth step. In the third growth step (Part III), the structure was grown at 650°C to minimize the thermal interdiffusion in the QD active layer. p- and n-type doping were obtained by using carbon and silicon, respectively. In addition to the InGaAsN QD laser structure, an InGaAs QW laser structure was also grown as a reference in the same way except for switching off the N precursor during growth of the InGaAs QW. After growth, the as-grown wafers were then processed into the standard ridge-waveguide laser diodes (LDs) with a stripe width of 4 μm and a cavity length varying from 500 to 1600 μm. Both facets of the LD were as-cleaved. Diodes were then characterized by photocurrent (PC), electroluminescence (EL), and light output power *vs.* current (L-I) measurements. During the PC measurements, the light from a tungsten-filament lamp is spectrally resolved through a monochromator before being focused on the front facet of the laser device, and the current was measured through an external circuit. The L-I characterization was performed under pulsed condition with a pulse width of 2 μs and a repetition rate of 28 kHz.

Results and Discussion

Figure 1 shows a typical RT L-I curve of an InGaAsN QD LD. The cavity length and the stripe width were 800 and 4 μm, respectively. An atomic force microscope (AFM) image of a reference InGaAsN QD sample without capping layer is also shown in the inset. The lateral size and the density of these dots were about 35 nm and 5×10^{10} cm^{-2}, respectively. The threshold current density (J_{th}) computed for 4 μm wide stripe devices with no correction for lateral current spreading was about 13 kA/cm^2 and the slope efficiency was about 0.29 W/A.

We also found that the J_{th} increased with increasing cavity length instead of decreasing which is normally observed for the semiconductor LDs. These results strongly suggest the overwhelming influence of nonradiative recombination in the QD structure, which is expected to increase with the increasing device length. This conclusion is also supported by the plot of z against J (injection current density) in which z lies in the range of 1-1.5 (not shown here),

* Electrochemical Society Active Member.
[z] E-mail: gao109@rsphysse.anu.edu.au

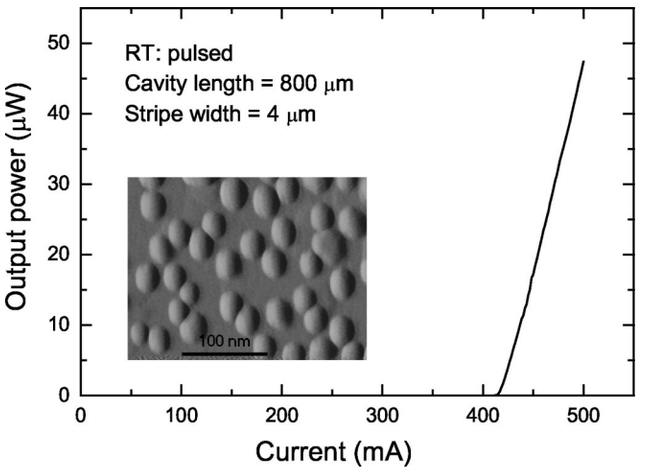

Figure 1. Light *vs.* current characteristics of an InGaAsN QD laser at RT under pulsed operation. The AFM image of surface InGaAsN QDs grown under the same condition as the LD structure is also shown in the inset.

where $z = \ln(I)/\ln(L^{1/2})$ for the spontaneous regime range before lasing occurs. The power measurement is taken from the side of the device in order to minimize the absorption in the semiconductor. If $z = 1$ the nonradiative recombination is dominant, and if $z = 2$ the dominant recombination mechanism is radiative due to bimolecular recombination.[20] This nonradiative recombination is most likely due to defects caused by nitrogen incorporation or dislocations caused by the mismatch strain.

The lasing spectrum and spontaneous emissions from the InGaAsN QD LDs obtained from EL measurements are shown in Fig. 2. For comparison, a PC spectrum at 0 V external bias is also shown. The LD used here is as cleaved with a cavity length of 800 μm and a stripe width of 4 μm. It is clearly seen that lasing occurs at about 450 mA at RT. At very low current injection levels, such as 50 mA, the maximum of the spontaneous emission is at about 1168 nm at RT. However, the emission wavelength shifts to 1078 nm when lasing takes place. This behavior is typical for a QD active region that provides enough gain for lasing only after the occupation rate of excited states becomes important, due to the limited volume of the QDs.[8,21] The 90 nm blueshift in wavelength between the lasing

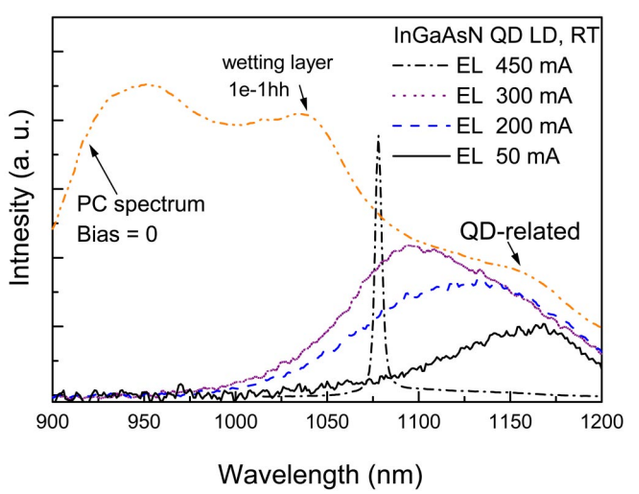

Figure 2. EL spectra at different injection current for an InGaAsN QD LD at RT. The PC spectrum at zero external bias is also shown for comparison and is shifted vertically for clarity.

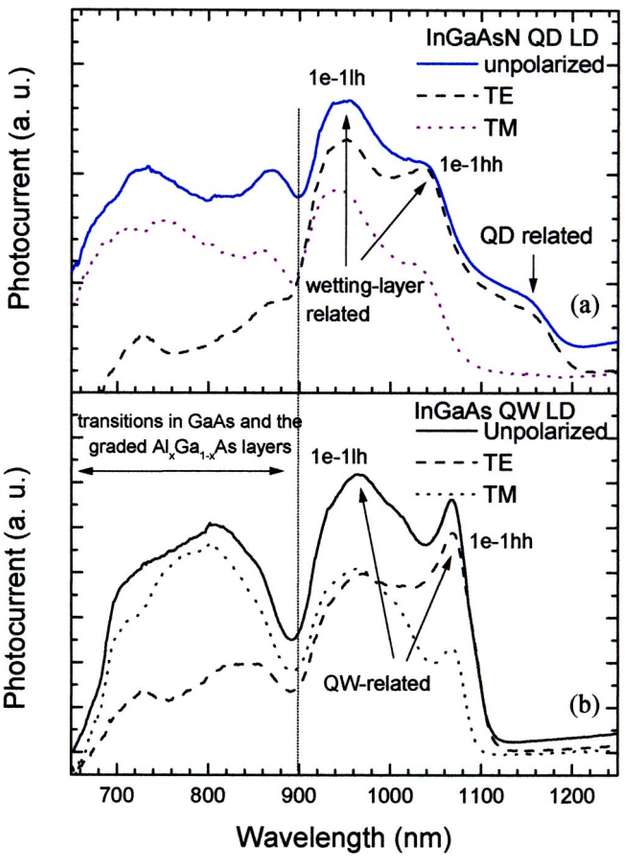

Figure 3. RT PC spectra at zero external bias of (a) an InGaAsN QD LD and (b) an reference InGaAs QW. Unpolarized light and lights with TE or TM polarization were used in these measurements. Both devices have a stripe width of 4 μm and a cavity length of about 1 mm.

emission and the peak of spontaneous emission implies that the device is lasing from the transitions related to an excited state in QDs. This is further supported from the comparison between the lasing spectrum and the PC spectrum shown in Fig. 2, where the lasing wavelength is 40 nm longer than the 1e-1hh transition in the wetting layer, implying that the lasing action is not due to the transitions in the wetting layer.

The PC spectra taken at 0 V external bias give insight into the transition strength of the QDs relative to the wetting layer and the contribution of heavy hole/light hole to the transition. Figure 3 shows such spectra measured at RT with polarized (TE or TM) and unpolarized light for the InGaAsN QD and InGaAs QW LDs. The common transitions in the wavelength range of 700-870 nm in these spectra belong to either the GaAs barriers or the graded $Al_xGa_{1-x}As$ surrounding the active region. In addition to these common features, there is an obvious difference between the QD (Fig. 3a) and the QW structures (Fig. 3b). The QD structure exhibits a low-energy signal ~1170 nm which is not seen in the QW structure and is attributed to transitions within the dots. This signal is much lower in intensity and broader than the QW or the wetting-layer peaks due to the smaller volume occupied by the QDs relative to the QW. This signal also reveals an almost flat absorption in the dots until a continuous background merges with the absorption peak of the wetting layer. Although not being observed in exactly the same way, a broad background PC signal from a InAs/GaAs QD structure was reported in Ref. 22. A high continuum background was also observed by Vasanelli *et al.* in the PC spectrum from a InAs/GaAs QD structure and was attributed to the cross transitions between the discrete dot levels and the unlocalized states in the wetting or barrier layers.[23]

Moreover, the dot transitions are clearly TE-polarized, which means that these transitions are mainly due to emissions from the electronic levels to the heavy hole states. Similarly, emissions from the electronic levels to the heavy hole (hh) states and to the light hole (lh) states in the wetting layer of the InGaAsN QD structure (Fig. 3a) or in the InGaAs QW structure (Fig. 3b) can be easily distinguished by comparing the TE mode and the TM mode photocurrent spectra. These transitions are indicated in Fig. 3. It can also be seen that PC peaks of the wetting layer in the QD structure are broader than those of the QW structure, which indicates a rougher interface between the wetting layer and the GaAs barriers, due to the QD formation.

Conclusion

In this work, we have demonstrated a room-temperature operation of InGaAsN QD ridge-waveguide edge emitting lasers grown on the GaAs substrate by MOCVD. InGaAsN QD LDs lased at 1078 nm from an excited state in QDs at RT. Photocurrent spectra of InGaAsN QD lasers revealed an almost flat absorption in the dots. The results of this work indicate that InGaAsN QDs have a great potential for long-wavelength semiconductor lasers.

Acknowledgment

The authors thank the Commonwealth Department of Education, Science and Training, and the Australian Research Council for their financial support.

References

1. M. Kondow, K. Uomi, A. Niwa, T. Kitatani, S. Watahiki, and Y. Yazawa, *Jpn. J. Appl. Phys., Part 1*, **35**, 1273 (1996).
2. T. Kitatani, K. Nakahara, M. Kondow, K. Uomi, and T. Tanaka, *Jpn. J. Appl. Phys., Part 2*, **39**, L86 (2000).
3. M. Fischer, M. Reinhardt, and A. Forchel, *IEEE Photonics Technol. Lett.*, **12**, 1313 (2000).
4. N. Tansu, N. J. Kirsch, and L. J. Mawst, *Appl. Phys. Lett.*, **81**, 2523 (2002).
5. N. Tansu, A. Quandt, M. Kanskar, W. Mulhearn, and L. J. Mawst, *Appl. Phys. Lett.*, **83**, 18 (2003).
6. Y. Arakawa and H. Sakaki, *Appl. Phys. Lett.*, **40**, 939 (1982).
7. M. Asada, M. Miyamoto, and Y. Suematsu, *IEEE J. Quantum Electron.*, **22**, 1915 (1986).
8. D. L. Huffaker, G. Park, Z. Zou, O. B. Shchekin, and D. G. Deppe, *Appl. Phys. Lett.*, **73**, 2564 (1998).
9. K. Mukai, Y. Nakata, K. Otsubo, M. Sugawara, N. Yokoyama, and H. Ishikawa, *IEEE Photonics Technol. Lett.*, **11**, 1205 (1999).
10. R. Sellin, C. Ribbat, M. Grundmann, N. N. Ledentsov, and D. Bimberg, *Appl. Phys. Lett.*, **78**, 1207 (2001).
11. N. Kirstaedter, O. G. Schmidt, N. N. Ledentsov, D. Bimberg, V. M. Ustinov, A. Y. Egorov, A. E. Zhukov, M. V. Maximov, P. S. Kop'ev, and Z. I. Alferov, *Appl. Phys. Lett.*, **69**, 1226 (1996).
12. O. B. Shchekin, J. Ahn, and D. G. Deppe, *Electron. Lett.*, **38**, 712 (2002).
13. S. Makino, T. Miyamoto, T. Kageyama, N. Nishiyama, F. Koyama, and K. Iga, *J. Cryst. Growth*, **221**, 561 (2000).
14. K. C. Yew, S. F. Yoon, Z. Z. Sun, and S. Z. Wang, *J. Cryst. Growth*, **247**, 279 (2003).
15. M. Sopanen, H. P. Xin, and C. W. Tu, *Appl. Phys. Lett.*, **76**, 994 (2000).
16. Q. Gao, H. H. Tan, L. Fu, and C. Jagadish, *Appl. Phys. Lett.*, **84**, 4950 (2004).
17. M. Buda, J. Hay, H. H. Tan, J. Wong-Leung, and C. Jagadish, *IEEE J. Quantum Electron.*, **39**, 625 (2003).
18. D. J. Friedman, J. F. Geisz, S. R. Kurtz, J. M. Olson, and R. Reedy, *J. Cryst. Growth*, **195**, 438 (1998).
19. R. Bhat, C. Caneau, L. Salamanca-Riba, W. Bi, and C. Tu, *J. Cryst. Growth*, **195**, 427 (1998).
20. A. J. Bennett, P. N. Stavrinou, C. Roberts, R. Murray, G. Parry, and J. S. Roberts, *J. Appl. Phys.*, **92**, 6215 (2002).
21. K. Mukai, N. Ohtsuka, M. Sugawara, and S. Yamazaki, *Jpn. J. Appl. Phys., Part 2*, **33**, L1710 (1994).
22. P. W. Fry, I. E. Itskevich, S. R. Parnell, J. J. Finley, L. R. Wilson, K. L. Schumacher, D. J. Mowbray, M. S. Skolnick, M. Al-Khafaji, A. G. Cullis, M. Hopkinson, J. C. Clark, and G. Hill, *Phys. Rev. B*, **62**, 16784 (2000).
23. A. Vasanelli, R. Fereira, and G. Bastard, *Phys. Rev. Lett.*, **89**, 2168041 (2002).